NASA TECHNICAL NOTE

NASA TN D-4401

NASA TN D-4401

EVALUATION OF BOUNDARY-LAYER AND WAKE-SURVEY DATA-REDUCTION TECHNIQUES IN COMPRESSIBLE FLOWS

by K. R. Czarnecki and Russell B. Sorrells III

Langley Research Center
Langley Station, Hampton, Va.

NATIONAL AERONAUTICS AND SPACE ADMINISTRATION • WASHINGTON, D. C. • APRIL 1968

EVALUATION OF BOUNDARY-LAYER AND WAKE-SURVEY DATA-REDUCTION TECHNIQUES IN COMPRESSIBLE FLOWS

By K. R. Czarnecki and Russell B. Sorrells III

Langley Research Center
Langley Station, Hampton, Va.

NATIONAL AERONAUTICS AND SPACE ADMINISTRATION

For sale by the Clearinghouse for Federal Scientific and Technical Information
Springfield, Virginia 22151 – CFSTI price $3.00

EVALUATION OF BOUNDARY-LAYER AND WAKE-SURVEY DATA-REDUCTION TECHNIQUES IN COMPRESSIBLE FLOWS

By K. R. Czarnecki and Russell B. Sorrells III
Langley Research Center

SUMMARY

An analytical and experimental investigation has been made of boundary-layer and wake-survey data-reduction techniques in compressible flows where the local Mach number just outside the boundary layer or wake at the measuring station does not match the average free-stream or normalizing value. The analytical study was limited to turbulent boundary layers with no heat transfer and to a Mach number range from 0 to 10. The experimental portion of the investigation was confined to zero-heat-transfer turbulent-wake surveys made behind a swept wing at free-stream Mach numbers of 1.61 and 2.01.

Results of the analytical boundary-layer calculations indicate that if simplified data-reduction techniques that neglect the deviation of the local Mach number from the average free-stream or normalizing value are utilized, sizable differences in momentum, displacement, and velocity thicknesses are incurred over much of the Mach number range for relatively small deviations in the local-flow characteristics or parameters. In general, use of the free-stream Mach number as a base both for determining velocity defects due to skin friction and for normalizing the thickness parameters, will introduce larger differences than use of local Mach number as the base for both items and interpretation of results as being obtained under stream conditions. Experimental wake data indicate that because of increased wake widths and reduced viscous heating or compressibility effects in comparison with boundary layers of equal momentum deficiency, the use of the free-stream-flow technique generally results in proportionately larger differences in wake-data reduction. With proper reservations for basic differences between wakes and boundary layers, the trends in the differences of the experimental wake data appear to be in good agreement with the analytical calculations for boundary-layer results which are reduced by the same method.

INTRODUCTION

During the experimental investigation by means of wake surveys of three-dimensional-wing skin-friction drag at supersonic speeds (ref. 1) an approximate

evaluation was made of the probable magnitude of the differences that might be incurred by the use of various methods of data reduction for the case where the flow conditions at the measuring station differ slightly from the desired reference conditions. This limited evaluation indicated the possibility of large differences under conditions where a cursory check of the accuracy of the basic wake-survey data would appear to justify the use of simplified data-reduction techniques. It thus appeared desirable to investigate this possibility of large differences in calculated boundary-layer parameters in greater detail.

For convenience, a basically analytical approach was chosen, which was, however, supplemented by a study of some experimental data. The analytical approach was limited to boundary layers inasmuch as the basic problem is pertinent in the reduction of boundary-layer data, and the theory for the development of wakes in compressible flows contains too many gaps (ref. 2) that cannot be handled analytically with any confidence. For further simplicity, the analysis was made for compressible-flow turbulent boundary layers with no heat transfer and a Prandtl number of 1, for boundary layers having power-law-type velocity profiles, and for isentropic free-stream flow. It should be recognized, nevertheless, that since similarities in the essential features of both laminar and turbulent boundary-layer flows exist, the trends derived from the turbulent boundary layers will also apply approximately to laminar boundary layers. Two types of approximate data-reduction techniques were studied. The boundary-layer parameters analyzed were the momentum, displacement, and velocity thicknesses. The Mach number range for the calculations was from 0 to 10. In the experimental study, some of the wake-survey data of reference 1, taken at varying distances downstream of the trailing edge of a sweptback wing at Mach numbers of 1.61 and 2.01, were reduced to momentum, displacement, and velocity thicknesses by the same methods; the results were assessed in terms of relative scatter and deviation from the results computed by the more correct reference method, which is described subsequently.

SYMBOLS

a to g	constants (defined by eqs. (33))
c_f	section skin-friction coefficient (defined by eq. (38))
c_s	section of wing chord
E	difference function (defined by eqs. (13) to (18))
M	Mach number

M_δ/M_∞ Mach number deviation ratio

m,p summation indices (see eqs. (33))

p static pressure (appendix C only)

n velocity-profile power-law parameter (defined by eq. (25))

u velocity in stream direction

u* velocity transformation variable (defined by eq. (B7))

x longitudinal distance downstream of wing trailing edge

y distance normal to surface

γ ratio of specific heat at constant pressure to specific heat at constant volume

δ total boundary-layer thickness

δ_u boundary-layer velocity thickness, $\int_0^\delta \left(1 - \frac{u}{u_r}\right)dy$

δ^* boundary-layer displacement thickness, $\int_0^\delta \left(1 - \frac{\rho u}{\rho_r u_r}\right)dy$

θ boundary-layer momentum thickness, $\int_0^\delta \frac{\rho u}{\rho_\infty u_\infty}\left(1 - \frac{u}{u_r}\right)dy$

ρ mass density of air

Subscripts:

r reference

δ local conditions outside boundary layer or wake except as noted in appendix C

δ_u boundary-layer velocity thickness

δ^* boundary-layer displacement thickness

θ boundary-layer momentum thickness

∞ free-stream conditions

Superscripts:

r reference method

A local-flow method

B free-stream flow method

THEORY

The basic problem, which is the subject of this paper, arises because the local stream conditions just outside a boundary layer at the measurement station are often not identical with the average or reference free-stream values owing to the existence of pressure gradients or other free-stream disturbances, and yet the differences are so small that there is a tendency to ignore them. For such conditions, it is assumed that the expressions for the losses within the boundary layer of momentum, mass flow, and velocity, respectively, can be determined from the local conditions as follows (see the shaded portions of sketches in fig. 1):

$$\int_0^\delta \rho u(u_\delta - u)dy \tag{1}$$

$$\int_0^\delta (\rho_\delta u_\delta - \rho u)dy \tag{2}$$

$$\int_0^\delta (u_\delta - u)dy \tag{3}$$

where u_δ is the local velocity just outside the boundary layer. Appendix A justifies the choice of the basic equations. If all the densities and velocities in equations (1) to (3) are divided by the reference free-stream values, these equations are derived:

$$\theta^r = \int_0^\delta \frac{\rho u}{\rho_\infty u_\infty}\left(\frac{u_\delta}{u_\infty} - \frac{u}{u_\infty}\right)dy \tag{4}$$

$$(\delta^*)^r = \int_0^\delta \left(\frac{\rho_\delta u_\delta}{\rho_\infty u_\infty} - \frac{\rho u}{\rho_\infty u_\infty}\right) dy \tag{5}$$

$$(\delta_u)^r = \int_0^\delta \left(\frac{u_\delta}{u_\infty} - \frac{u}{u_\infty}\right) dy \tag{6}$$

which are the approximately correct reference expressions for boundary-layer momentum, displacement, and velocity thickness normalized in terms of the average or reference free-stream quantities.

Often, because the differences between u_∞ and u_δ are very small, it has been assumed to be justifiable without explicit substantiation, to simplify the data-reduction procedure or to ignore these differences in the interpretation of the data. In one procedure the boundary-layer parameters are assumed to be expressed with sufficient accuracy completely in terms of local-stream-reference conditions. (See fig. 1.) This conversion is, of course, the correct procedure except that often the local conditions are not specified, and the data are presented as having been obtained under stream-flow conditions. The question thus arises as to how much of an error or difference will ensue if an attempt is made to correlate such data with those reported correctly. For this local-flow method, equations (4) to (6) convert to

$$\theta^A = \int_0^\delta \frac{\rho u}{\rho_\delta u_\delta}\left(1 - \frac{u}{u_\delta}\right) dy \tag{7}$$

$$(\delta^*)^A = \int_0^\delta \left(1 - \frac{\rho u}{\rho_\delta u_\delta}\right) dy \tag{8}$$

$$(\delta_u)^A = \int_0^\delta \left(1 - \frac{u}{u_\delta}\right) dy \tag{9}$$

In the other approach, it is assumed that with sufficient accuracy, ρ_∞ and u_∞ can be substituted for ρ_δ and u_δ. This procedure amounts to determining the momentum, mass-flow, and velocity losses corresponding to the Mach number losses shown by the shaded areas in figure 2, and neglects to isolate the changes in local velocities and densities induced by changes in the flow outside the boundary layer. For this free-stream-flow method, equations (4), (5), and (6) are modified to

$$\theta^B = \int_0^\delta \frac{\rho u}{\rho_\infty u_\infty}\left(1 - \frac{u}{u_\infty}\right) dy \tag{10}$$

$$(\delta^*)^B = \int_0^\delta \left(1 - \frac{\rho u}{\rho_\infty u_\infty}\right) dy \tag{11}$$

$$(\delta_u)^B = \int_0^\delta \left(1 - \frac{u}{u_\infty}\right) dy \tag{12}$$

In order to assess the possible magnitudes of the differences involved in making such simplifications, the following difference functions are defined:

$$E_\theta^A = \frac{\theta^A - \theta^r}{\theta^r} = \frac{\theta^A}{\theta^r} - 1 \tag{13}$$

$$E_{\delta^*}^A = \frac{(\delta^*)^A}{(\delta^*)^r} - 1 \tag{14}$$

$$E_{\delta_u}^A = \frac{(\delta_u)^A}{(\delta_u)^r} - 1 \tag{15}$$

$$E_\theta^B = \frac{\theta^B}{\theta^r} - 1 \tag{16}$$

$$E_{\delta^*}^B = \frac{(\delta^*)^B}{(\delta^*)^r} - 1 \tag{17}$$

$$E_{\delta_u}^B = \frac{(\delta_u)^B}{(\delta_u)^r} - 1 \tag{18}$$

where the subscript on the E defines the boundary-layer thickness parameter that is involved, and the superscript specifies the simplified basis on which the parameter is being calculated; that is, whether on local or free-stream Mach number for determining skin-friction momentum or other losses. Substitution of the integrals in equations (4) to (12) into equations (13) to (18) and the conversion of the normal distance variable y to y/δ yields

$$E_\theta^A = \frac{\int_0^1 \frac{\rho u}{\rho_\delta u_\delta}\left(1 - \frac{u}{u_\delta}\right) d\left(\frac{y}{\delta}\right)}{\int_0^1 \frac{\rho u}{\rho_\infty u_\infty}\left(\frac{u_\delta}{u_\infty} - \frac{u}{u_\infty}\right) d\left(\frac{y}{\delta}\right)} - 1 \tag{19}$$

$$E^{A}_{\delta^*} = \frac{\int_0^1 \left(1 - \frac{\rho u}{\rho_\delta u_\delta}\right) d\left(\frac{y}{\delta}\right)}{\int_0^1 \left(\frac{\rho_\delta u_\delta}{\rho_\infty u_\infty} - \frac{\rho u}{\rho_\infty u_\infty}\right) d\left(\frac{y}{\delta}\right)} - 1 \tag{20}$$

$$E^{A}_{\delta_u} = \frac{\int_0^1 \left(1 - \frac{u}{u_\delta}\right) d\left(\frac{y}{\delta}\right)}{\int_0^1 \left(\frac{u_\delta}{u_\infty} - \frac{u}{u_\infty}\right) d\left(\frac{y}{\delta}\right)} - 1 \tag{21}$$

$$E^{B}_{\theta} = \frac{\int_0^1 \frac{\rho u}{\rho_\infty u_\infty} \left(1 - \frac{u}{u_\infty}\right) d\left(\frac{y}{\delta}\right)}{\int_0^1 \frac{\rho u}{\rho_\infty u_\infty} \left(\frac{u_\delta}{u_\infty} - \frac{u}{u_\infty}\right) d\left(\frac{y}{\delta}\right)} - 1 \tag{22}$$

$$E^{B}_{\delta^*} = \frac{\int_0^1 \left(1 - \frac{\rho u}{\rho_\infty u_\infty}\right) d\left(\frac{y}{\delta}\right)}{\int_0^1 \left(\frac{\rho_\delta u_\delta}{\rho_\infty u_\infty} - \frac{\rho u}{\rho_\infty u_\infty}\right) d\left(\frac{y}{\delta}\right)} - 1 \tag{23}$$

$$E^{B}_{\delta_u} = \frac{\int_0^1 \left(1 - \frac{u}{u_\infty}\right) d\left(\frac{y}{\delta}\right)}{\int_0^1 \left(\frac{u_\delta}{u_\infty} - \frac{u}{u_\infty}\right) d\left(\frac{y}{\delta}\right)} - 1 \tag{24}$$

Solutions for equations (19) to (24) in closed, analytical form are obtained by assuming that the flow in the free stream is isentropic, and that the boundary layer has a power-law-type velocity profile

$$\frac{u}{u_\delta} = \left(\frac{y}{\delta}\right)^{1/n} \tag{25}$$

and a constant stagnation temperature equal to the free-stream value (zero heat transfer, Prandtl number equal to 1) which, with the aid of the thermal equation of state, yields the required density-velocity relationship:

$$\frac{\rho_\delta}{\rho} = 1 + \frac{\gamma - 1}{2} M_\delta^2 \left[1 - \left(\frac{u}{u_\delta}\right)^2\right] \tag{26}$$

Substitution of equations (25) and (26) into equations (19) to (24) result in (after simplification of the integrals, expansion, and conversion of some integrals into finite generalized series with a remainder term, and integration) the desired final expressions:

$$E_{\theta}^{A} = \left(\frac{M_{\infty}}{M_{\delta}}\right)^{2}\left(\frac{b}{e}\right)^{\frac{\gamma}{\gamma-1}} - 1 \tag{27}$$

$$E_{\delta^*}^{A} = \frac{M_{\infty}}{M_{\delta}}\left(\frac{b}{e}\right)^{\frac{\gamma+1}{2(\gamma-1)}} - 1 \tag{28}$$

$$E_{\delta_u}^{A} = \frac{M_{\infty}}{M_{\delta}}\left(\frac{b}{e}\right)^{1/2} - 1 \tag{29}$$

$$E_{\theta}^{B} = \left[\frac{M_{\infty}}{M_{\delta}}\left(\frac{b}{e}\right)^{1/2} - 1\right]\left\{\frac{\frac{c^{n-1}}{2}(f - g) - \sum_{m=1}^{m=p}\frac{c^{2(m-1)}}{n - 2m + 1}}{\frac{c^{n-1}}{2}\left[(c + 1)f + (c - 1)g + 1 - (-1)^{n}\right] - \sum_{m=1}^{m=p}\frac{c^{2(m-1)}}{(n - 2m + 2)(n - 2m + 1)}}\right\} \tag{30}$$

$$E_{\delta^*}^{B} = \left[\frac{M_{\infty}}{M_{\delta}}\left(\frac{b}{e}\right)^{\frac{\gamma+1}{2(\gamma-1)}} - 1\right]\left\{\frac{1}{1 - \frac{n}{a}\left[\frac{c^{n-1}}{2}(f - g) - \sum_{m=1}^{m=p}\frac{c^{2(m-1)}}{n - 2m + 1}\right]}\right\} \tag{31}$$

$$E_{\delta_u}^{B} = \left[\frac{M_{\infty}}{M_{\delta}}\left(\frac{b}{e}\right)^{1/2} - 1\right](n + 1) \tag{32}$$

where

$$\left.\begin{aligned} a &= \frac{\gamma - 1}{2}M_{\delta}^{2} \\ b &= 1 + a = 1 + \frac{\gamma - 1}{2}M_{\delta}^{2} \\ c &= \sqrt{\frac{b}{a}} \end{aligned}\right\} \tag{33}$$

(Equations continued on next page)

$$
\left.
\begin{aligned}
d &= \frac{\gamma - 1}{2} M_\infty{}^2 \\
e &= 1 + d = 1 + \frac{\gamma - 1}{2} M_\infty{}^2 \\
f &= (-1)^n \left(\log_e |c + 1| - \log_e |c| \right) \\
g &= \log_e |c - 1| - \log_e |c| \\
m &= 1, 2, 3, 4, \ldots \\
p &= \frac{1}{2} \left\{ n - \frac{1}{2} \left[1 - (-1)^n \right] \right\}
\end{aligned}
\right\} \tag{33}
$$

Because of the limitations imposed by the method of evaluating some of the integrals, the exponential parameter n is restricted to whole numbers in equations (30) and (31). An illustration of the methods used in obtaining solutions is presented in appendix B. Where the free-stream Mach number is 0, equations (27) to (32) reduce to

$$E_\theta^A = \left(\frac{M_\infty}{M_\delta} \right)^2 - 1 \tag{34}$$

$$E_{\delta^*}^A = E_{\delta_u}^A = \frac{M_\infty}{M_\delta} - 1 \tag{35}$$

$$E_\theta^B = \left(\frac{M_\infty}{M_\delta} - 1 \right) (n + 2) \tag{36}$$

$$E_{\delta^*}^B = E_{\delta_u}^B = \left(\frac{M_\infty}{M_\delta} - 1 \right) (n + 1) \tag{37}$$

RESULTS AND DISCUSSION

Boundary-Layer Theory

To assess the probable magnitudes of the differences to be expected in the use of the two simplified methods for reducing boundary-layer survey data to the various boundary-layer thicknesses, some calculations were made of the difference functions (eqs. (27) to (32)) for a range of the basic parameters M_∞, M_δ/M_∞, and n. The free-stream Mach number was varied from 0 to 10; the parameter M_δ/M_∞ signifying the

magnitude of the difference between the local and free-stream Mach numbers was varied from 1.00 to 1.05; and the value of the exponential factor n was varied from 6 to 14. An n of 6 corresponds to fully turbulent boundary layers at low Reynolds numbers and to values just above the conditions for transition from laminar to turbulent flow. An n of 14 corresponds to very high Reynolds numbers, probably on the order of 10^9 or more. The results of the calculations where the boundary-layer thicknesses are evaluated completely in terms of the local conditions are presented in figures 3 and 4. The results where the thicknesses are determined entirely in terms of the free-stream conditions are shown in figures 5 to 7.

Local-flow method.- As expected from the formulation of the problem, the difference functions determined by the local-flow method (eqs. (27) to (29)) are independent of the shape of the boundary-layer velocity profiles (figs. 3 and 4). For M_δ/M_∞ constant and greater than 1, the difference functions are all negative at the lower free-stream Mach numbers, but E_θ^A and $E_{\delta^*}^A$ become positive and $E_{\delta_u}^A$ approaches 0 at the higher Mach numbers (fig. 3). This tendency toward more positive difference values with increasing M_∞ is generally very rapid at the lower free-stream Mach numbers (0.5 to 4.0), but much slower as M_∞ approaches 10 because of the close approach to the asymptotic limits existing for $M_\infty = \infty$. These trends result from the fact that M_δ/M_∞, which has been taken as the basic deviation function, and the various functions of b/e, which represent changes in local static pressure and local speed of sound, are opposing terms in isentropic flow because, physically, increases in M_δ cause decreases in p_δ and the local speed of sound. As M_∞ approaches zero, the changes in p_δ and the local speed of sound from the assumed deviation of M_δ from M_∞ become small and the Mach number deviation term M_δ/M_∞ has the dominant effect. (See eqs. (34) and (35) for $M_\infty = 0$.) As M_∞ approaches 10, the changes in p_δ and the local speed of sound resulting from the assumed deviation are very large and become the dominating factors in the difference terms E_θ^A and $E_{\delta^*}^A$, and become essentially canceling terms in the case of $E_{\delta_u}^A$.

The results presented in figure 4 indicate that the difference terms are nearly linear functions of the deviation ratio M_δ/M_∞, within the limits of the calculations presented herein. No calculations were made for M_δ less than M_∞. For equal deviations in this direction, the difference functions would be nearly identical numerically to those shown in figures 3 and 4, except that the positive and negative signs would be reversed.

Figures 3 and 4 show that a deviation of M_δ of only 1 percent ($M_\delta/M_\infty = 1.01$) will cause a difference in the calculation of the parameters θ^A, $(\delta^*)^A$, and $(\delta_u)^A$ of about -2, -1, and -1 percent, respectively, as M_∞ approaches 0, and will cause differences of about 5, 5, and nearly 0 percent, respectively, as M_∞ approaches 10. For

larger deviations the differences will be proportionately larger (within the range of calculations). For a small range of Mach number, near 1.4 for θ^A and 1.0 for $(\delta^*)^A$, the difference in calculating these parameters is small because of the aforementioned change in sign of the difference functions. In view of the relatively large differences that may be involved over large portions of the free-stream Mach number range in reducing boundary-layer survey data to the various thickness parameters by this local-flow method if the local-flow conditions do not match the desired free-stream reference values, it appears desirable always to specify the local-flow conditions under which the measurements were made.

Free-stream-flow method.- Where the boundary-layer thickness parameters are computed entirely in terms of the average free-stream conditions (free-stream-flow method) the values of the difference functions become dependent upon the boundary-layer velocity profiles (figs. 5 to 7) or on the power-profile parameter n. For M_δ/M_∞ constant and greater than 1 the difference functions are again all negative at M_∞ near zero. As M_∞ increases, E^B_θ and $E^B_{\delta_u}$ tend toward zero asymptotically, the most rapid changes occurring in the Mach number range from about 0 to 4. The difference function $E^B_{\delta^*}$ becomes positive for $M_\infty > 1$, reaches a peak value in the Mach number range from about 3 to 4, and then declines gradually as M_∞ increases toward 10.

The results presented in figures 6 and 7 indicate that the difference terms are nearly linear functions of the deviation ratio M_δ/M_∞ and of the exponential parameter n for the range of these parameters studied herein. The differences become larger as n increases as a result of the relative shrinking of the low-density region near the wall. This decrease in the low-density region causes an increase in the mass-flow and velocity weighting factors involved in calculating the difference functions.

Again, no calculations were made for $M_\delta < M_\infty$. For equal deviations in this direction the difference functions would be nearly identical numerically to those shown in figures 5 to 7, except that the signs would be reversed.

An inspection of figures 5 to 7 indicates that a deviation in M_δ of only 1 percent from the average free-stream value M_∞ will result in calculation differences by the use of the free-stream-flow technique in determining the various thickness parameters of -7 to -16 percent at $M_\infty = 0$, -7 to 13 percent at $M_\infty = 3$, and -1 to 7 percent at $M_\infty = 10$. For larger deviations in M_δ/M_∞ the differences are proportionately larger. The large differences that may be incurred make the use of this data-reduction method undesirable at any time.

The difference curves just discussed illustrate the extreme importance of determining and specifying M_δ accurately. The assumption is made that the boundary-layer Mach number profile has been well defined experimentally except that an insufficient

number of points were taken external to the boundary layer, perhaps because of strongly rotational external flow, to determine M_δ with great accuracy. As a consequence, the local Mach number external to the boundary layer was erroneously equated to M_∞ although in reality it was 1 percent higher. Then the experimenter will incur differences of the magnitude indicated in figures 5 to 7 although he may actually be trying to use the local-flow method in reducing the data. The seriousness of the problem is emphasized if it is recognized that even the determination of M_δ to within $\pm 1/4$ percent accuracy, which requires sophisticated instrumentation and testing techniques, can still result in maximum differences up to 3 and 4 percent for some conditions.

Experimental Wake Results

The results of the experimental investigation are presented in table I. The basic data were derived from the wake surveys of reference 1. These data apply only to station 2 of wings F (a flat wing) and 1 (a linearly twisted wing) and only for an angle of attack of 0°. Station 2 was the only one at which wake surveys were made at several locations downstream of the wing, and restrictions of the analysis to the aforementioned wings at zero incidence eliminate the involvement of separated flows. Turbulent boundary-layer flow was assured by fixing transition near the wing leading edges. Complete details of instrumentation and testing techniques can be found in reference 1.

Raw wake-survey data were reduced to thickness parameters by the three methods discussed under "Theory": the reference method, the local-flow method, and the free-stream-flow method. All methods, as applied, allowed for a variable M_δ through the wake and for measured changes in local static pressure. For convenience, the reference method expressions for boundary-layer (and wake) momentum, displacement, and velocity thickness are presented in appendix C in a form most suitable for usual data-reduction procedures. Variable M_δ values were determined by the fairing of a fictitious, linear pitot pressure tangential to the experimental values determined just outside either side of the wake. More details of this technique can be found in reference 1. Calculations indicate, however, that for the data incorporated in this report, both the effects of skewness of M_δ and of variable local static pressure in the direction normal to the wake were negligible. In table I, only the momentum thicknesses have been averaged, inasmuch as within the simplifications incorporated into the basic reference equations (eqs. (4) to (6)), this parameter can remain constant as the wake expands downstream of the wing. Displacement and velocity thicknesses, however, still must decrease so that the parameters δ^*/θ and δ_u/θ approach 1 at very large distances downstream of the wing.

Examination of the momentum thicknesses obtained by use of the reference method shows that the maximum scatter for the stations downstream of any one wing at one test Mach number was ± 3.4 percent and that the average maximum scatter for all test

conditions was on the order of ±2 percent. An analysis of all pertinent factors suggests that the biggest contributor to this scatter is probably the inability to determine M_δ with any greater accuracy. In fact, approximate calculations indicate that errors in M_δ on the order of ±0.002 could account for nearly all the experimental differences, and it is doubtful that the accuracy of M_δ exceeds this figure. The average maximum scatter at $M_\infty = 2.01$ is somewhat less than that at $M_\infty = 1.61$ and follows the trend indicated in figure 5, but the indication may be fortuitous because of the insufficient size of the experimental sample. The consistency of the nearly 3-percent increase in θ^r of wing 1 over wing F at both test Mach numbers suggests that the indication of at least the trend may be meaningful, but again the sample is small. Finally, both theoretical calculations and the tendency of the experimental data to follow the trends derived on the isentropic-flow basis appear to indicate that the wing trailing-edge shock did not have a major influence in these tests if the wake data were properly referenced to stream-flow conditions.

Inspection of the momentum-thickness results obtained by the local-flow method indicates a maximum scatter distribution nearly identical with that obtained by the reference method. The existence of this pattern is ascribed primarily to small errors in the determination of M_δ. At $M_\infty = 1.61$, M_δ is usually less than M_∞, and θ^A, according to the theoretical isentropic-flow calculations, should be slightly less than θ^r (see fig. 3 and reverse sign), but experimentally the reverse is true. This difference in trend is attributed to the wing trailing-edge shock losses existing in the experimental flow and the relatively small isentropic-flow effects to be expected at this test Mach number. Furthermore, the difference is so small that it is well within experimental error. At $M_\infty = 2.01$, θ^A increases over θ^r, as expected from the theoretical isentropic-flow calculations, and again this difference indicates the relative smallness of nonisentropic-shock effects. Although the apparent difference in the use of the local-flow method in reducing the data of these experimental results, as compared with the reference method, is practically nonexistent at $M_\infty = 1.61$ and relatively small (a little over 2 percent on the average) at $M_\infty = 2.01$, it can be very significant at higher Mach numbers. (See fig. 3 again.) These differences between methods again indicate the need for specifying the flow conditions under which the wake data were obtained even if the difference from the stream or average reference condition is small.

Calculations of the momentum thickness by the free-stream-flow method result in very large scatter. The distribution of momentum thickness with downstream measuring station is no longer primarily random in character as it was for θ^r and θ^A, but is dependent upon the relative magnitude of M_δ compared with M_∞. The magnitude of the scatter is considerably larger than that expected from the boundary-layer calculations of figure 5. This trend is due to the fact that the wake is two to three times as wide as a boundary layer having an equal momentum deficiency; and it can be readily inferred from figure 2 that as the Mach number deficiency becomes more shallow and spreads to

several times the boundary-layer thickness, the effects of deviations of M_δ from M_∞ become proportionately more significant. Analysis also shows that as the Mach number deficiency shallows in the central part of the wake relative to the Mach number deficiency in the boundary layer close to the wall, the viscous heating or compressibility effects in the wake decrease relative to those computed for the boundary layer and, in effect, the wake difference functions become more equivalent to the boundary-layer difference functions which were computed for lower free-stream Mach numbers. For θ^B this effect will result in increasing errors for the wake relative to the boundary layer at the same M_∞. (See fig. 5.) The scatter in θ^B is much larger at $M_\infty = 2.01$ than at $M_\infty = 1.61$. This trend is primarily the result of the relatively larger deviations experienced in M_δ at $M_\infty = 2.01$, but part of the increased scatter can also be traced to the aforementioned decreased compressibility effects for the wake relative to the boundary layer. This effect is stronger at $M_\infty = 2.01$ than at $M_\infty = 1.61$.

At this point it is of interest to compare for this single wing test station the experimental section skin-friction coefficients derived from the average momentum thickness which were computed by the reference method with the theoretical values. (See table II.) Experimental coefficients were determined from

$$c_f = \frac{2(\theta^r)_{average}}{c_s} \tag{38}$$

The theoretical values were computed by the Sommer and Short reference temperature method (ref. 3), and the comparison shows that the experimental skin-friction coefficients exceed the theoretical values by about 4 to 9 percent. A preliminary analysis indicates that this trend probably cannot be ascribed to effects of the transition-fixing roughness strip alone.

An analysis of the displacement- and velocity-thickness results obtained in this experimental phase of the investigation is not presented in detail. It should suffice to state that this set of results conforms to the theoretical isentropic-flow boundary-layer calculations, with reservations for differences in wakes and boundary layers, in the same manner as the momentum thickness data. The only notable effect was that the decreased compressibility effects for the wake relative to the boundary layer resulted in considerably smaller scatter for $(\delta^*)^B$ than might have been inferred from the theoretical boundary-layer calculations which neglect this effect.

CONCLUDING REMARKS

An analytical and experimental investigation has been made of boundary-layer and wake-survey data-reduction techniques in compressible flows where the local Mach

number just outside the boundary layer or wake does not match the average free-stream or normalizing value. The analytical investigation was limited to turbulent boundary layers with no heat transfer and to a Mach number range from 0 to 10. The experimental portion of the investigation was confined to zero-heat-transfer turbulent-wake surveys made behind a swept wing at free-stream Mach numbers of 1.61 and 2.01.

Results of the analytical boundary-layer calculations indicate that if simplified data-reduction techniques that neglect the deviation of the local Mach number from the average free-stream or normalizing value are utilized, sizable differences in momentum, displacement, and velocity thicknesses are incurred over much of the Mach number range, for relatively small deviations in the local-flow characteristics or parameters. In general, use of the free-stream Mach number as a base both for determining velocity defects due to skin-friction and for normalizing the thickness parameters, introduces larger differences than use of local Mach numbers as the base for both items and interpretation of the results as being obtained under stream conditions. Experimental wake data indicate that, because of increased wake widths and reduced viscous heating or compressibility effects compared with boundary layers of equal momentum deficiency, the use of the free-stream-flow technique generally results in proportionately larger differences in wake-data reduction. With proper reservations for basic differences between wakes and boundary layers, the trends in the differences of the experimental wake data appear to be in good agreement with the analytical calculations for boundary-layer results which were reduced by the same method.

Langley Research Center,
National Aeronautics and Space Administration,
Langley Station, Hampton, Va., October 19, 1967,
126-13-02-11-23.

APPENDIX A

CHOICE OF BASIC EQUATIONS

The assumption that the boundary-layer momentum, mass flow, and velocity defects in a flow with pressure gradients can be expressed by equations (1) to (3) neglects the fact that the reference quantities ρ_δ and u_δ vary along the length of the boundary layer ahead of the measuring station. For thin wings the variation in the reference quantities is small. Furthermore, at supersonic speeds the decreases in u_δ and increases in ρ_δ experienced on the forward portions of the wing are partially compensated for by the reversed effects encountered on the rear parts of the wing. Thus, the overall effects are generally assumed to be relatively small. However, the objective of this paper is not to investigate this problem, but to determine the possible magnitude of differences that are incurred in reducing or interpreting the data, if, the boundary layer having been formed and measured, the reference conditions at the measuring station are misinterpreted or misapplied because the differences between local and free-stream conditions are believed to be negligibly small. For such an investigation, equations (1) to (3) should be adequate. For the estimation of skin friction on wings from wake surveys in pressure gradients, the variation of ρ_δ and u_δ along the wake could affect the results. Comparison of theoretical calculations made herein with suitable experimental results can show whether the omission of detailed variation of the reference quantities is of great significance. Simplified theoretical computations indicate that for the experimental data reported herein, the maximum effect is less than 2 percent and the average effect is considerably less.

APPENDIX B

EXAMPLE OF SOLUTION OF EQUATIONS

The equation for the difference function of the boundary-layer displacement thickness computed on the assumption that the free-stream values of p_∞ and u_∞ can be substituted for ρ_δ and u_δ is

$$E^B_{\delta^*} = \frac{\int_0^1 \left(1 - \frac{\rho u}{\rho_\infty u_\infty}\right) d\left(\frac{y}{\delta}\right)}{\int_0^1 \left(\frac{\rho_\delta u_\delta}{\rho_\infty u_\infty} - \frac{\rho u}{\rho_\infty u_\infty}\right) d\left(\frac{y}{\delta}\right)} \tag{B1}$$

With the conversion of the terms in equation (B1) to a common denominator, the addition and subtraction of the term $\rho_\delta u_\delta / \rho_\infty u_\infty$ in the integrand of the numerator of the equation, and the multiplication of the denominator only by the identity term $\rho_\delta u_\delta / \rho_\delta u_\delta$, equation (B1) is transformed into

$$E^B_{\delta^*} = \frac{\int_0^1 \left(\frac{\rho_\infty u_\infty - \rho_\delta u_\delta + \rho_\delta u_\delta - \rho u}{\rho_\infty u_\infty}\right) d\left(\frac{y}{\delta}\right) - \int_0^1 \left(\frac{\rho_\delta u_\delta - \rho u}{\rho_\infty u_\infty}\right) d\left(\frac{y}{\delta}\right)}{\int_0^1 \left(\frac{\rho_\delta u_\delta}{\rho_\infty u_\infty}\right)\left(\frac{\rho_\delta u_\delta - \rho u}{\rho_\delta u_\delta}\right) d\left(\frac{y}{\delta}\right)} \tag{B2}$$

The integrals can now be broken up to yield

$$E^B_{\delta^*} = \left(\frac{\rho_\infty u_\infty}{\rho_\delta u_\delta} - 1\right) \frac{\int_0^1 d\left(\frac{y}{\delta}\right)}{\int_0^1 d\left(\frac{y}{\delta}\right) - \int_0^1 \frac{\rho u}{\rho_\delta u_\delta} d\left(\frac{y}{\delta}\right)} \tag{B3}$$

The term $\rho_\infty u_\infty / \rho_\delta u_\delta$ is converted into a more convenient form by the use of the usual (ref. 4) isentropic-flow relationships (an assumption that precludes free-stream shock losses) and the result is

$$\frac{\rho_\infty u_\infty}{\rho_\delta u_\delta} = \frac{M_\infty}{M_\delta}\left(\frac{b}{e}\right)^{\frac{\gamma+1}{2(\gamma-1)}} \tag{B4}$$

where

$$b = 1 + \frac{\gamma - 1}{2} M_\delta^2$$

APPENDIX B

$$e = 1 + \frac{\gamma - 1}{2} M_\infty^2$$

Obviously,

$$\int_0^1 d\left(\frac{y}{\delta}\right) = 1 \tag{B5}$$

In order to evaluate the integral

$$\int_0^1 \frac{\rho u}{\rho_\delta u_\delta} d\left(\frac{y}{\delta}\right) \tag{B6}$$

however, some assumptions have to be made about the boundary layer. It was first assumed that the boundary layer had a power-type velocity profile that could be represented by a new variable u^*, where

$$u^* = \frac{u}{u_\delta} = \left(\frac{y}{\delta}\right)^{1/n} \tag{B7}$$

Also, the static pressure through the boundary layer was assumed to be constant and equal to the value just outside the boundary layer (compatible only with zero or small pressure gradients) and the stagnation temperature within the boundary layer was assumed to be constant and equal to the free-stream value (equivalent to zero heat transfer, Prandtl number equal to 1). These assumptions allow the derivation, with the aid of the thermal equation of state, of the required density-velocity relationship

$$\frac{\rho_\delta}{\rho} = 1 + \frac{\gamma - 1}{2} M_\delta^2 \left[1 - \left(\frac{u}{u_\delta}\right)^2\right] \tag{B8}$$

Substitution of equations (B7) and (B8) into equation (B6) results in

$$\int_0^1 \frac{\rho u}{\rho_\delta u_\delta} d\left(\frac{y}{\delta}\right) = \frac{n}{a} \int_0^1 \frac{u^{*n}}{c^2 - u^{*2}} du^* \tag{B9}$$

where

$$a = \frac{\gamma - 1}{2} M_\delta^2$$

$$b = 1 + a = 1 + \frac{\gamma - 1}{2} M_\delta^2$$

$$c = \sqrt{\frac{b}{a}}$$

Expansion of the integrand on the right-hand side of equation (B9) and conversion of the result into a finite generalized series with a remainder term that is compatible for both even and odd values of n result in the equation

APPENDIX B

$$\int_0^1 \frac{\rho u}{\rho_\infty u_\infty} d\left(\frac{y}{\delta}\right) = \frac{n}{a}\int_0^1 \left\{ -\sum_{m=1}^{m=p} c^{2(m-1)} u^{*n-2m} + \frac{\frac{c^n}{2}\left[1 + (-1)^n\right] + \frac{c^{n-1}}{2}\left[1 - (-1)^n\right]u^*}{c^2 - u^{*2}} \right\} du^* \tag{B10}$$

where

$$m = 1, 2, 3, 4, \ldots$$

$$p = \frac{1}{2}\left\{n - \frac{1}{2}\left[1 - (-1)^n\right]\right\}$$

and which can now be readily integrated to yield

$$\int_0^1 \frac{\rho u}{\rho_\delta u_\delta} d\left(\frac{y}{\delta}\right) = \frac{n}{a}\left[\frac{c^{n-1}}{2}(f - g) - \sum_{m=1}^{m=p} \frac{c^{2(m-1)}}{n - 2m + 1}\right] \tag{B11}$$

where

$$f = (-1)^n\left(\log_e|c + 1| - \log_e|c|\right)$$

$$g = \log_e|c - 1| - \log_e|c|$$

Substitution of equations (B5) and (B11) into equation (B3) results in the desired final expression

$$E^B_{\delta^*} = \left[\frac{M_\infty}{M_\delta}\left(\frac{b}{e}\right)^{\frac{\gamma+1}{2(\gamma-1)}} - 1\right]\left\{1 - \frac{n}{a}\left[\frac{c^{n-1}}{2}(f - g) - \sum_{m=1}^{m=p} \frac{c^{2(m-1)}}{n - 2m + 1}\right]\right\}^{-1} \tag{B12}$$

Because of the limitations imposed by the method of evaluating the integral of equation (B9), the power-law parameter n is restricted to whole numbers in equation (B12).

APPENDIX C

COMPUTATIONAL FORM OF THE REFERENCE BOUNDARY-LAYER- OR WAKE-THICKNESS PARAMETERS

The reference expressions (where local-flow conditions at the measuring station do not match the desired free-stream normalizing values) for boundary-layer (and wake) momentum, displacement, and velocity thicknesses for conditions of no heat transfer and constant stagnation temperature through the boundary layer equal to the free-stream value are, in the form most suitable for usual data-reduction procedures,

$$\theta^r = \int_0^\delta \frac{p_\delta}{p_\infty} \frac{M}{M_\infty} \frac{M_\delta}{M_\infty} \left(\sqrt{\frac{1 + \frac{\gamma - 1}{2} M^2}{1 + \frac{\gamma - 1}{2} M_\delta^2}} - \frac{M}{M_\delta} \right) dy \tag{C1}$$

$$(\delta^*)^r = \int_0^\delta \frac{p_\delta}{p_\infty} \frac{M_\delta}{M_\infty} \sqrt{\frac{1 + \frac{\gamma - 1}{2} M_\delta^2}{1 + \frac{\gamma - 1}{2} M_\infty^2}} \left(1 - \frac{M}{M_\delta} \sqrt{\frac{1 + \frac{\gamma - 1}{2} M^2}{1 + \frac{\gamma - 1}{2} M_\delta^2}} \right) dy \tag{C2}$$

$$(\delta_u)^r = \int_0^\delta \frac{M_\delta}{M_\infty} \sqrt{\frac{1 + \frac{\gamma - 1}{2} M_\infty^2}{1 + \frac{\gamma - 1}{2} M_\delta^2}} \left(1 - \frac{M}{M_\delta} \sqrt{\frac{1 + \frac{\gamma - 1}{2} M_\delta^2}{1 + \frac{\gamma - 1}{2} M^2}} \right) dy \tag{C3}$$

In equations (C1) to (C3) p_δ and M_δ are not necessarily the local static pressure and local Mach number at the outer edge of the boundary layer but can be variable quantities if gradients in these terms are in the "potential flow" outside the boundary layer and normal to the surface. In such instances M_δ normally has to be estimated by some extrapolation or interpolation process as described in this paper and in reference 1. Also, the assumption has been made that the local static pressure has been measured and can be variable. For constant static pressure through the boundary layer, p_δ becomes constant and equal to the value ascribed to the edge of the boundary layer; for constant or uniform local free-stream flow, M_δ becomes constant and equal to the local Mach number just outside the boundary layer. Under these conditions the ratios involving only terms in p_δ and p_∞ and M_δ and M_∞ can be taken outside the integral sign if desired. As indicated by the wake experimental results presented in the body of this

paper and by approximate theoretical estimates, the error in using these simplified equations in place of the more complex and usually unsolvable fully correct equations is negligible over the usual range of test conditions to which they may be applied.

REFERENCES

1. Sorrells, Russell B., III; Jackson, Mary W.; and Czarnecki, K. R.: Measurement by Wake Momentum Surveys at Mach 1.61 and 2.01 of Turbulent Boundary-Layer Skin Friction on Five Swept Wings. NASA TN D-3764, 1966.

2. Schubauer, Galen B.; and Tchen, C. M.: Free Turbulent Flows. Turbulent Flows and Heat Transfer. Vol. V of High Speed Aerodynamics and Jet Propulsion, C. C. Lin, ed., Princeton Univ. Press, 1959, pp. 158-184.

3. Sommer, Simon C.; and Short, Barbara J.: Free-Flight Measurements of Turbulent-Boundary-Layer Skin Friction in the Presence of Severe Aerodynamic Heating at Mach Numbers From 2.8 to 7.0. NACA TN 3391, 1955.

4. Ames Research Staff: Equations, Tables, and Charts for Compressible Flow. NACA Rept. 1135, 1953. (Supersedes NACA TN 1428.)

TABLE I.- CALCULATION OF WING WAKE PARAMETERS

(a) Dimensional quantities in inches

Station, x/c_s	Mach number			Wake parameters											
				Reference method				Local-flow method				Free-stream method			
	M_∞	M_δ	Difference, percent	θ^r, in.	Scatter in θ^r, percent (a)	$(\delta^*)^r$, in.	$(\delta_u)^r$, in.	θ^A, in.	Scatter in θ^A, percent (a)	$(\delta^*)^A$, in.	$(\delta_u)^A$, in.	θ^B, in.	Scatter in θ^B, percent (a)	$(\delta^*)^B$, in.	$(\delta_u)^B$, in.
Wing F															
0.25	1.610	1.586	-1.5	0.0398		0.0926	0.0545	0.0400		0.0920	0.0550	0.0442		0.0894	0.0597
.50	1.610	1.601	-.6	.0372		.0828	.0466	.0374		.0830	.0468	.0395		.0843	.0492
.62	1.610	1.609	-.1	.0377		.0830	.0459	.0378		.0831	.0458	.0377		.0856	.0459
.87	1.610	1.591	-1.2	.0390		.0841	.0451	.0391		.0837	.0456	.0490		.0744	.0558
				[b].0384	$b_{\pm 3.4}$			[b].0386	$b_{\pm 3.3}$			[b].0426	$b_{\pm 8.0}$		
Wing 1															
0.25	1.610	1.591	-1.2	0.0407		0.0950	0.0560	0.0407		0.0943	0.0563	0.0476		0.0876	0.0635
.62	1.610	1.610	0.0	.0387		.0855	.0476	.0388		.0860	.0476	.0383		.0908	.0472
.87	1.610	1.610	0.0	.0388		.0841	.0456	.0389		.0844	.0456	.0388		.0894	.0456
				[b].0394	$b_{\pm 2.5}$			[b].0395	$b_{\pm 2.4}$			[b].416	$b_{\pm 10.8}$		
Wing F															
0.25	2.010	2.018	0.4	0.0363		0.1082	0.0551	0.0371		0.1107	0.0551	0.0342		0.1337	0.0528
.62	2.010	2.036	1.3	.0359		.1020	.0475	.0367		.1050	.0471	.0289		.1351	.0395
.87	2.010	2.055	2.2	.0364		.1022	.0460	.0374		.1063	.0455	.0242		.1368	.0342
				[b].0362	$b_{\pm 0.6}$			[b].0371	$b_{\pm 0.9}$			[b].0291	$b_{\pm 26.0}$		
Wing 1															
0.25	2.010	2.089	0.9	0.0379		0.1125	0.0560	0.0383		0.1142	0.0558	0.0313		0.1331	0.0488
.62	2.010	2.046	1.8	.0363		.1039	.0484	.0370		.1067	.0479	.0287		.1284	.0394
.87	2.010	2.064	2.7	.0374		.1053	.0471	.0381		.1089	.0465	.0156		.1519	.0253
				[b].0372	$b_{\pm 2.1}$			[b].378	$b_{\pm 2.0}$			[b].252	$b_{\pm 33.5}$		

[a]Scatter is based on mean of high and low values of θ.

[b]Average values.

TABLE I.- CALCULATION OF WING WAKE PARAMETERS – Concluded

(b) Dimensional quantities in centimeters

Station, x/c_s	Mach number			Wake parameters											
				Reference method				Local-flow method				Free-stream method			
	M_∞	M_δ	Difference, percent	θ^r, cm	Scatter in θ^r, percent (a)	$(\delta^*)^r$, cm	$(\delta_u)^r$, cm	θ^A, cm	Scatter in θ^A, percent (a)	$(\delta^*)^A$, cm	$(\delta_u)^A$, cm	θ^B, cm	Scatter in θ^B, percent (a)	$(\delta^*)^B$, cm	$(\delta_u)^B$, cm
Wing F															
0.25	1.610	1.586	-1.5	0.1011		0.2352	0.1384	0.1016		0.2337	0.1397	0.1123		0.2271	0.1516
.50	1.610	1.601	-.6	.0945		.2103	.1184	.0950		.2108	.1189	.1003		.2141	.1250
.62	1.610	1.609	-.1	.0958		.2108	.1166	.0960		.2111	.1163	.0958		.2174	.1166
.87	1.610	1.591	-1.2	.0991		.2136	.1146	.0993		.2126	.1158	.1245		.1890	.1417
				[b].0975	[b]±3.4			[b].0980	[b]±3.3			[b].1082	[b]±8.0		
Wing 1															
0.25	1.610	1.591	-1.2	0.1034		0.2413	0.1422	0.1034		0.2395	0.1430	0.1209		0.2225	0.1613
.62	1.610	1.610	0.0	.0983		.2172	.1209	.0986		.2184	.1209	.0973		.2306	.1199
.87	1.610	1.610	0.0	.0986		.2136	.1158	.0988		.2144	.1158	.0986		.2271	.1158
				[b].1001	[b]±2.5			[b].1003	[b]±2.4			[b].1056	[b]±10.8		
Wing F															
0.25	2.010	2.018	0.4	0.0922		0.2748	0.1400	0.0942		0.2812	0.1400	0.0869		0.3396	0.1341
.62	2.010	2.036	1.3	.0912		.2591	.1207	.0932		.2667	.1196	.0734		.3432	.1003
.87	2.010	2.055	2.2	.0925		.2596	.1168	.0950		.2700	.1156	.0615		.3475	.0869
				[b].0919	[b]±0.6			[b].0941	[b]±0.9			[b].0739	[b]±26.0		
Wing 1															
0.25	2.010	2.029	0.9	0.0963		0.2858	0.1422	0.0973		0.2901	0.1417	0.0795		0.3381	0.1240
.62	2.010	2.046	1.8	.0922		.2639	.1229	.0940		.2710	.1217	.0729		.3261	.1001
.87	2.010	2.064	2.7	.0950		.2675	.1196	.0968		.2766	.1181	.0396		.3858	.0643
				[b].0945	[b]±2.1			[b].0960	[b]±2.0			[b].0640	[b]±33.5		

[a]Scatter is based on mean of high and low values of θ.

[b]Average values.

TABLE II.- COMPARISON OF CORRECT EXPERIMENTAL SKIN FRICTION WITH THEORY

Wing	Mach number	Section skin-friction coefficient, c_f		Difference, percent
		Experimental	Theoretical	
F	1.61	0.00610	0.00587	3.9
1	1.61	.00625	.00587	6.5
F	2.01	.00573	.00540	6.1
1	2.01	.00590	.00540	9.3

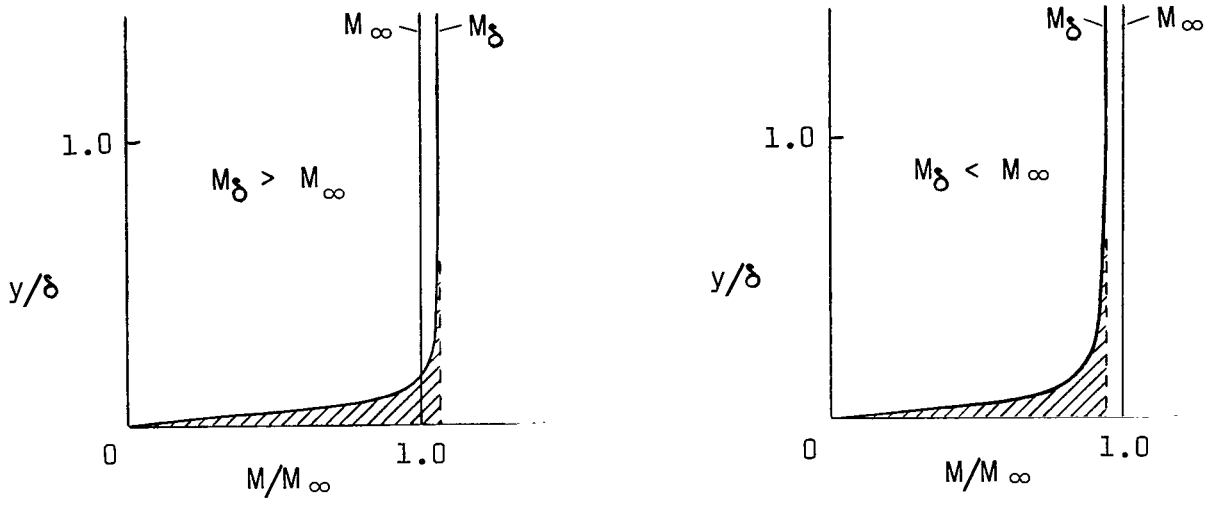

Figure 1.- Portions of boundary layer affected in calculation of losses of momentum, mass flow, and velocity with local Mach number as base.

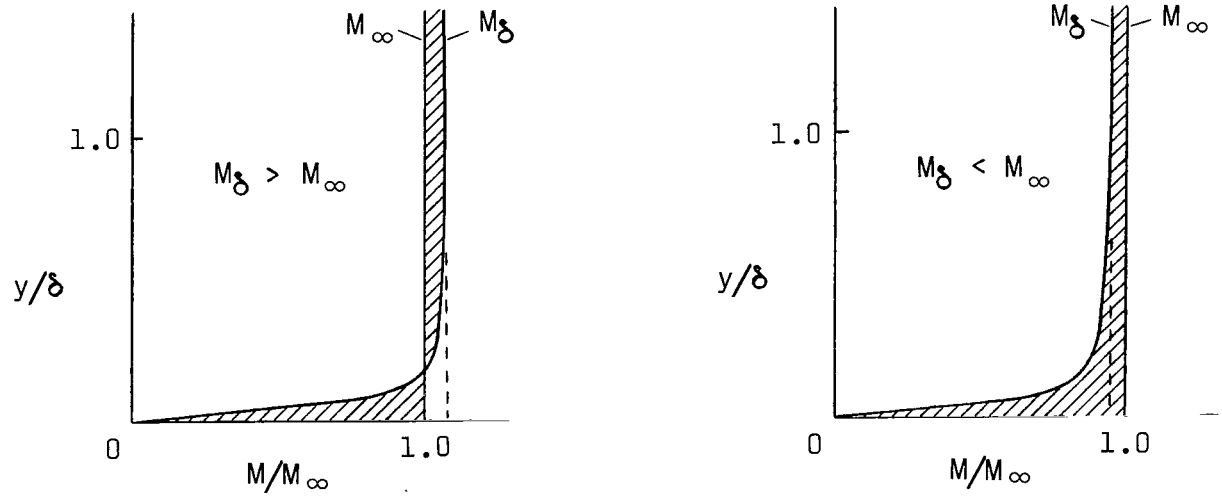

Figure 2.- Portions of boundary layer affected in calculation of losses of momentum, mass flow, and velocity with free stream as base.

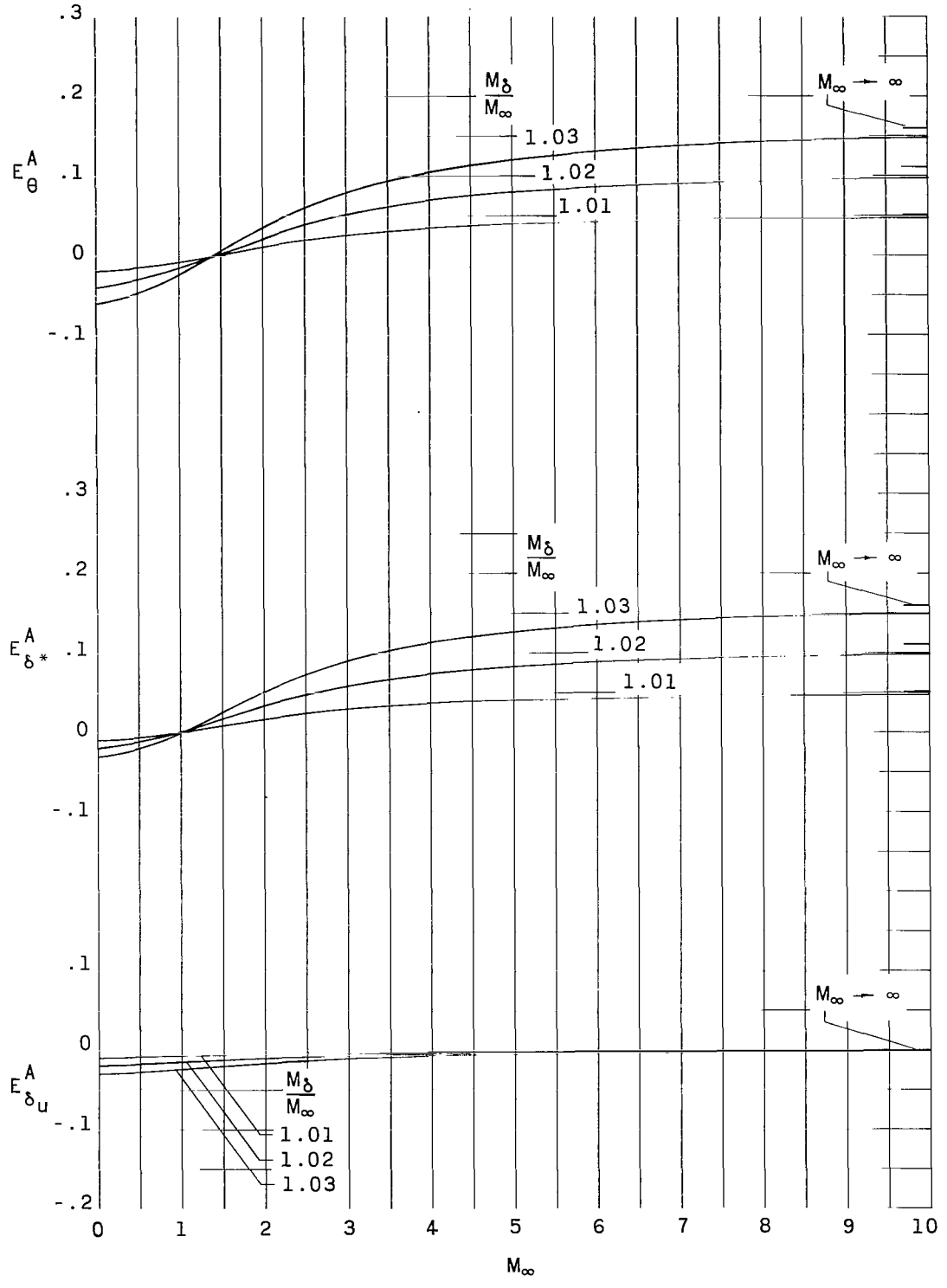

Figure 3.- Variation of the difference functions E^A_θ, $E^A_{\delta^*}$, and $E^A_{\delta_u}$ with M_∞.

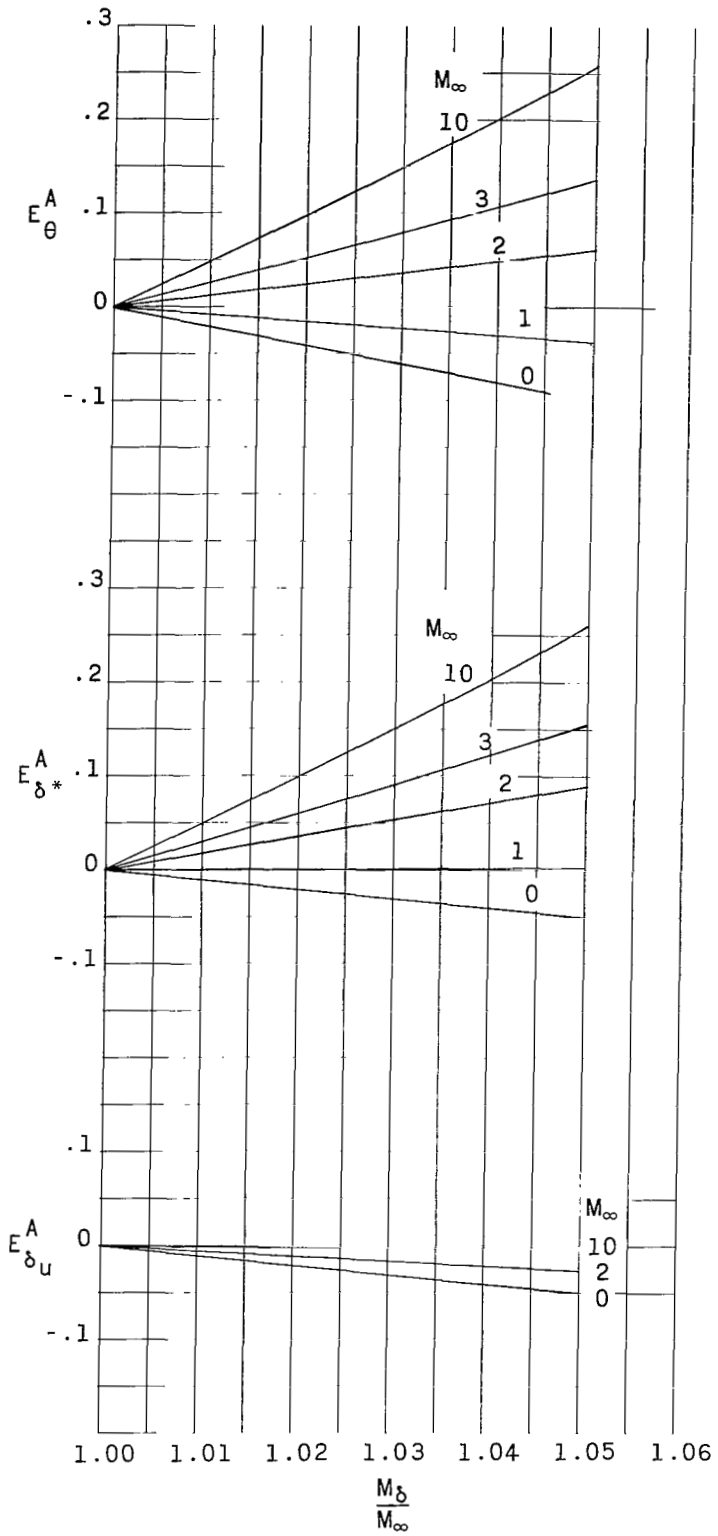

Figure 4.- Variation of the difference functions E^A_θ, $E^A_{\delta^*}$ and $E^A_{\delta_u}$ with $\frac{M_\delta}{M_\infty}$.

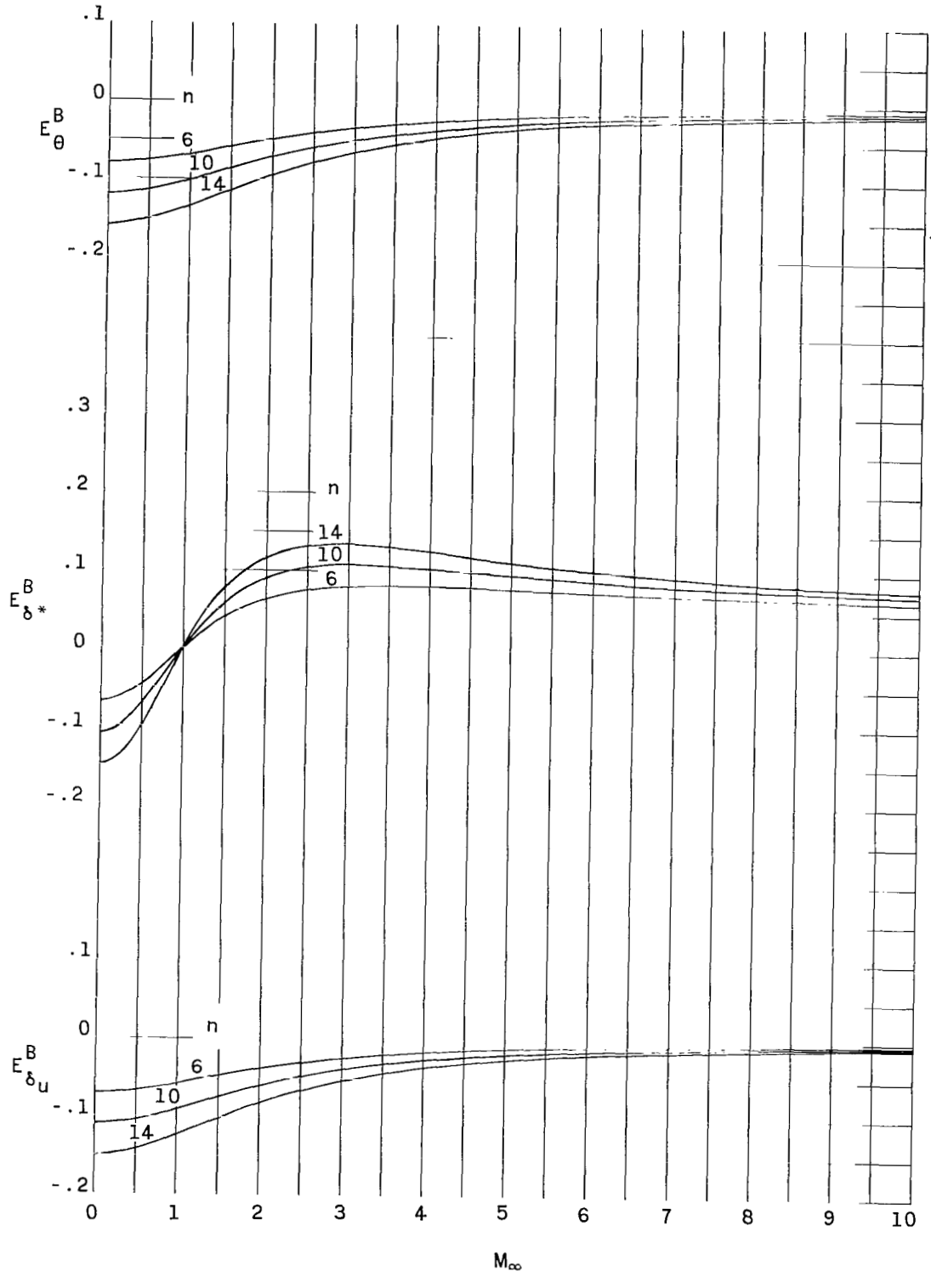

Figure 5.- Variation of the difference functions E^B_θ, $E^B_{\delta^*}$, and $E^B_{\delta_u}$ with M_∞. $\frac{M_\delta}{M_\infty} = 1.01$.

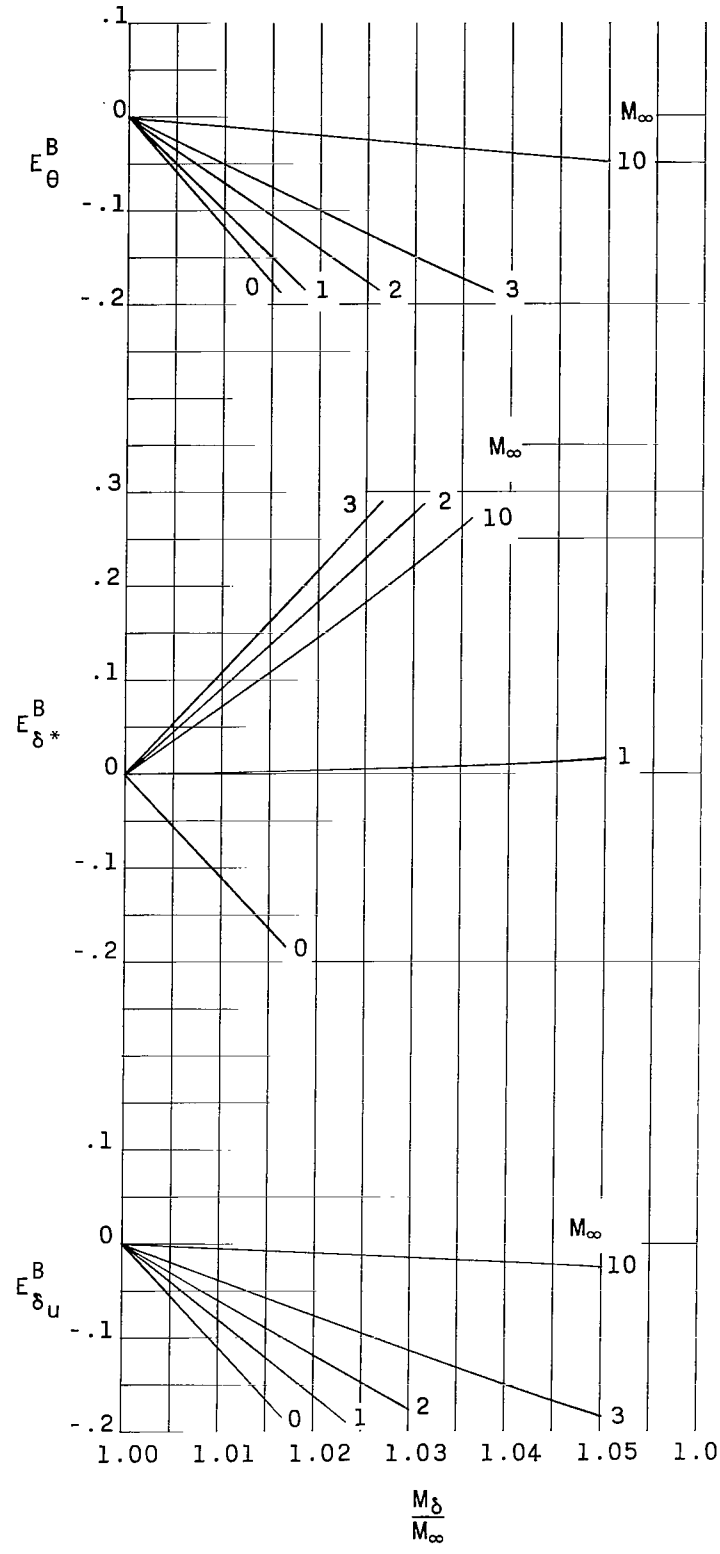

Figure 6.- Variation of the difference functions E^B_θ, $E^B_{\delta^*}$, and $E^B_{\delta_u}$ with $\frac{M_\delta}{M_\infty}$. n = 10.

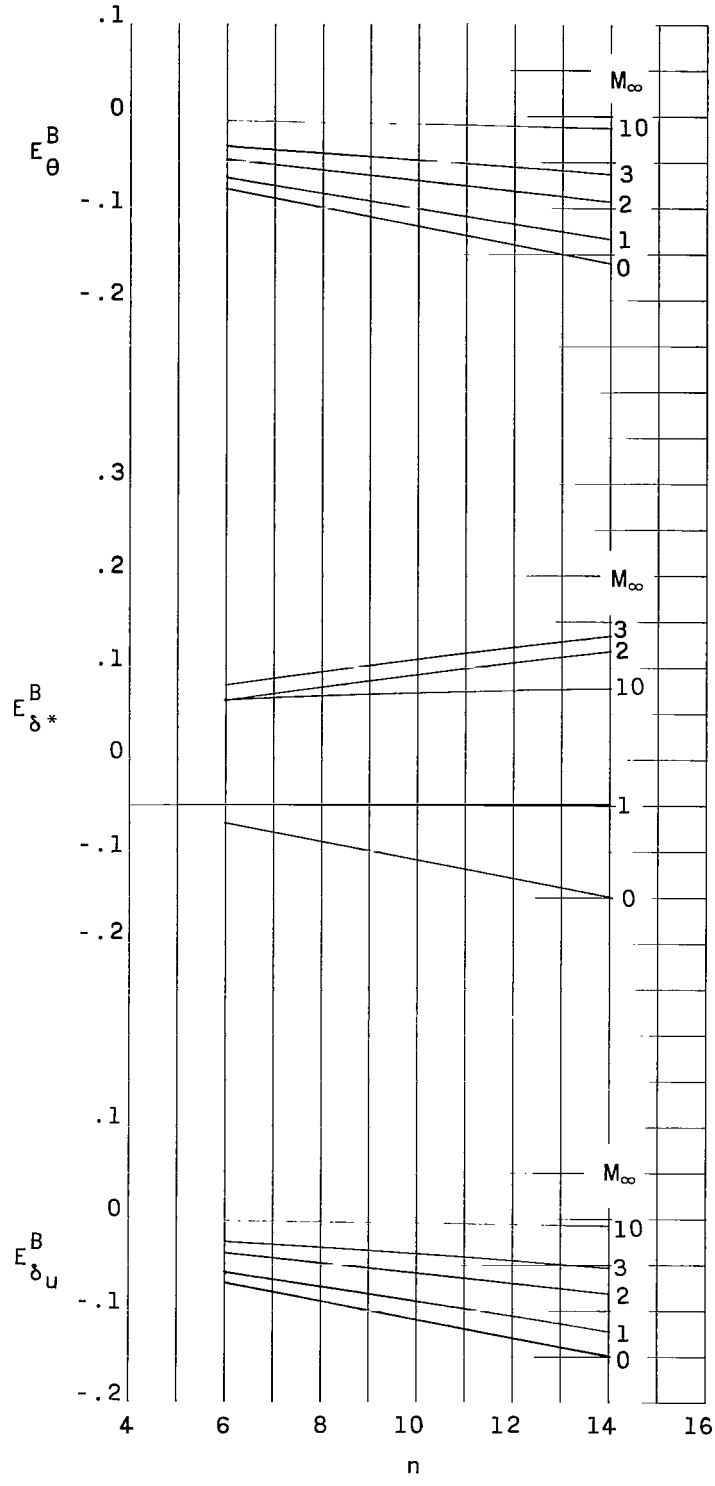

Figure 7.- Variation of the difference functions E^B_θ, $E^B_{\delta^*}$, and $E^B_{\delta_u}$ with n. $\frac{M_\delta}{M_\infty} = 1.01$.

National Aeronautics and Space Administration
WASHINGTON, D. C.

OFFICIAL BUSINESS

FIRST CLASS MAIL

POSTAGE AND FEES PAID
NATIONAL AERONAUTICS AN
SPACE ADMINISTRATION

"The aeronautical and space activities of the United States shall be conducted so as to contribute . . . to the expansion of human knowledge of phenomena in the atmosphere and space. The Administration shall provide for the widest practicable and appropriate dissemination of information concerning its activities and the results thereof."

—NATIONAL AERONAUTICS AND SPACE ACT OF 1958

NASA SCIENTIFIC AND TECHNICAL PUBLICATIONS

TECHNICAL REPORTS: Scientific and technical information considered important, complete, and a lasting contribution to existing knowledge.

TECHNICAL NOTES: Information less broad in scope but nevertheless of importance as a contribution to existing knowledge.

TECHNICAL MEMORANDUMS: Information receiving limited distribution because of preliminary data, security classification, or other reasons.

CONTRACTOR REPORTS: Scientific and technical information generated under a NASA contract or grant and considered an important contribution to existing knowledge.

TECHNICAL TRANSLATIONS: Information published in a foreign language considered to merit NASA distribution in English.

SPECIAL PUBLICATIONS: Information derived from or of value to NASA activities. Publications include conference proceedings, monographs, data compilations, handbooks, sourcebooks, and special bibliographies.

TECHNOLOGY UTILIZATION PUBLICATIONS: Information on technology used by NASA that may be of particular interest in commercial and other non-aerospace applications. Publications include Tech Briefs, Technology Utilization Reports and Notes, and Technology Surveys.

Details on the availability of these publications may be obtained from:

SCIENTIFIC AND TECHNICAL INFORMATION DIVISION

NATIONAL AERONAUTICS AND SPACE ADMINISTRATION

Washington, D.C. 20546